Budapest University of Technology and Economics

Faculty of Civil Engineering

Department of Structural Mechanics

EFFECT OF PREBUCKLING DEFORMATIONS ON THE LATERAL TORSIONAL BUCKLING OF DOUBLY SYMMETRIC BEAMS: INFLUENCE OF TORSIONAL RIGIDITY, END SUPPORTS, AND INTERMEDIATE SUPPORTS

SUMMARY

GHAITH ABU REDEN

Supervised by

Dr. Sándor Ádány

Budapest, 2025

1. Introduction

Classical solutions for lateral torsional buckling (LTB) consider a perfect beam when the buckling occurs, neglecting prebuckling deformations. However, previous studies [1-13] show that the primary (in-plane) deflections might influence the solution of LTB. There seems to be a consensus in the available literature that the prebuckling deformations increase the critical moment, and that the increase is dominantly determined by the lateral rigidity of the beam. However, available literature is not too numerous and is limited to the most basic case (forked supports with open cross sections). Furthermore, discrepancies can be found in the given formulae. This research is focused on understanding the role of prebuckling deflections on LTB in depth by understanding the details of derivations done in the literature and extending on it by investigating the role of torsional rigidity [AGA1, AGA4], end supports [AGA2, AGA5, AGA6], and intermediate lateral supports and beam length [AGA3, AGA7].

2. The basic case: analytical derivations

The first case to be considered is a beam with simple forked supports, uniform moment distribution, and no intermediate lateral supports. This is referred to as the "basic case", which is mostly discussed in the literature. First, a literature review on the available literature was conducted, and several observations were made. For instance, it was found that most papers agree that the increase due to prebuckling deflections can be expressed by the $1/\sqrt{1-I_y/I_x}$ factor, with I_y being the weak axis, and I_x the strong axis moment of inertia. More precise formulae are given in several papers, and there are small discrepancies between these formulae. Furthermore, it is implicitly assumed or explicitly stated in most papers that the provided formula to consider the prebuckling effect is generally valid. Discrepancies can also be found in the underlying basic mechanical-mathematical formulae. Finaly, there is hardly any attempt to use general numerical methods such as the shell finite element method.

The derivation is based on the energy method, where the total potential is expressed as the sum the strain energy, and the work of the stresses on the nonlinear strains. To define these terms, the first step is to define the shape functions. In case of LTB, the secondary displacements are the lateral translation and twisting rotation, u and φ (Fig. 1). The shape functions must satisfy the boundary conditions. The assumed displacement functions are simple half sinewaves, and the primary displacements can be expressed as a parabolic function (Fig. 1).

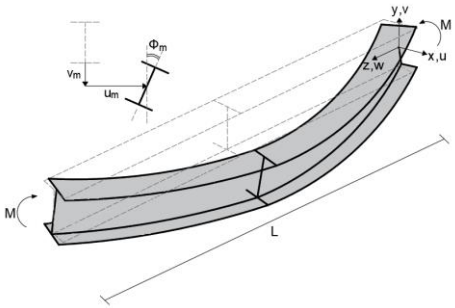

Figure 1: Coordinate system, displacements.

In the derivation, a transformation between the deformed and undeformed coordinate systems is needed to obtain the curvatures on the deformed geometry of the beam. One of the sources of discrepancies in the literature stems from the assumed transformation matrix, as several variants can be derived depending on what terms are eliminated or kept. Eliminating higher terms simplify the solution, but these must be chosen carefully not to affect the accuracy of the resulting formula. After determining the proper transformation matrix, the expressions for curvatures are established, depending on which transformation matrix is used, several curvature expressions can be derived as well. Again, the resulting expression for strain depends on the assumed transformation matrix, as well as approximations that can be made.

Depending on the simplifications employed in the derivations, several options for the critical moment formula can be identified (denoted as ‘a’, ‘b’, ‘c’, etc.). Another source of discrepancies is the section-related approximations. Four types of approximations are introduced here, referred to as ‘open’ and ‘open-simple’ for open cross sections (such as the doubly symmetric I section, DSI), and ‘closed’ and ‘closed simple’ for closed cross sections (such as rectangular hollow section, RHS). Even with these approximations, the final equation is of 4^{th}-degree. However, in the literature the higher-degree terms are always eliminated, and the critical moment is calculated from a simplified quadratic equation. Fig. 2 shows the solutions for the various resulting formulae for open and closed cross sections, respectively. It can be concluded that the introduced simplifications can lead to a significant scatter, hence the derivations should be done carefully to avoid errors. Later, further analytical derivations are performed for different end supports and intermediate supports. Since the approximations established by [3] were found to be suitable, they are used for these further studies.

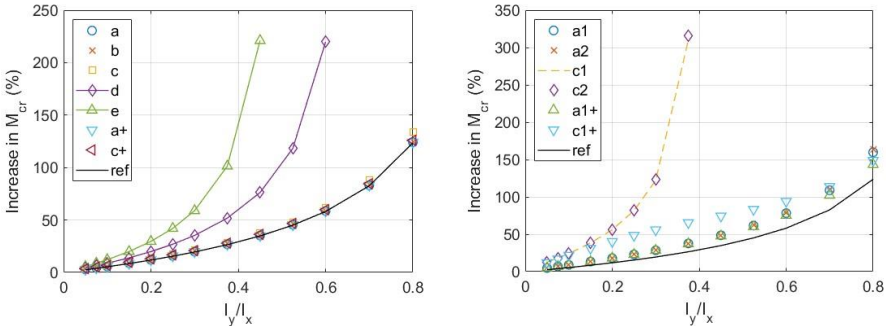

Figure 2: Moment increase due to prebucking deflection: open sections (left) and closed sections (right).

3. The effect of end supports

In this Chapter, single-span prismatic and originally straight girders are analyzed with doubly symmetric steel cross-sections. The beam is subjected to uniform moment about the major axis, and various boundary conditions have been considered. The critical moments without and with considering the in-plane deflections have been calculated (leading to M_{cr0} and M_{cr}, respectively). Analytical and numerical methods have been applied, as follows: (i) analytical formulae derived in Chapter 2, as well as further formulae for other boundary conditions derived in this chapter, (ii) Linear Buckling Analysis (LBA) analysis by beam FEM, (iii) LBA by shell FEM, (iv) Geometrically Nonlinear Analysis with Imperfections (GNIA) by beam FEM, and (v) GNIA by shell FEM.

Various classic boundary condition combinations have been considered. The main two variables are the rotation and warping. The notation used is: 'P' indicates a pinned/free condition, and 'F' indicates a fixed condition, while 'r' and 'w' specify whether the fixity is for rotation (about the minor axis *y*) or warping. For example: PrPw indicates an end where both the rotation and warping are free to occur, while PrFw indicates a free rotation and fixed warping, etc. The longitudinal translation is always prevented at one end, and the rotation about the major axis *x* is always free.

For the dimensions, in the case of DSI, the flange width is 200 mm, the flange and web thicknesses are 20 and 12 mm, respectively, while the total section depth (out-to-out) is a variable so that the I_y/I_x ratio would be in the range of 0.05 to 0.75. In the case of RHS, the section width is 150 mm, the flange and web thicknesses are 30 and

10 mm, respectively, the total section depth varies, so that the I_y/I_x ratio would be in the range of 0.03 to 0.75. For the material, a classic isotropic steel is considered, with a Young's modulus equal to 210000 MPa, and Poisson's ratio equal to 0.3.

- **Analytical solutions**

Critical moment formulae are derived for each support condition, both for open and closed cross sections. In the derivation, options 'open-simple' and 'closed-simple' are used, and the final equation is simplified to a quadratic equation. Critical moment formulae are initially derived assuming a single trigonometric term in the displacement functions, However, results of these formulae were inaccurate in certain cases, therefore, more refined formulae are derived, using 3 trigonometric terms. Table 1 shows the derived formulae (single term), where M_{cr0} is the critical moment without prebuckling deformations, while M_{cr} is with prebuckling deformations.

Table 1: Critical moment formulae for different boundary conditions.

Support Case	$M_{cr0,1t}$	$M_{cr,1t}$
FrFw-FrFw	$\frac{\pi}{0.5L}\sqrt{EI_y\left(GJ+\frac{\pi^2 EI_w}{(0.5L)^2}\right)}$	$M_{cr0,1t}\Big/\sqrt{\left(1-\frac{EI_y}{EI_x}\right)\left(1+2\frac{EI_y}{EI_x}\right)}$
FrPw-FrPw	$\frac{3\pi}{8}\frac{\pi}{0.5L}\sqrt{EI_y\left(GJ+\frac{\pi^2 EI_w}{L^2}\right)}$	$M_{cr0,1t}\Big/\sqrt{\left(1-\frac{EI_y}{EI_x}\right)\left(1+\left(\frac{9\pi^2}{16}-1\right)\frac{EI_y}{EI_x}\right)}$
PrFw-PrFw	$\frac{3\pi}{8}\frac{\pi}{L}\sqrt{EI_y\left(GJ+\frac{\pi^2 EI_w}{(0.5L)^2}\right)}$	$M_{cr0,1t}\Big/\sqrt{\left(1-\frac{EI_y}{EI_x}\right)\left(1+\frac{EI_y}{EI_x}\left(\frac{27\pi^2}{256}-1\right)\right)}$
PrPw-FrFw	$\frac{\pi}{0.6992L}\sqrt{EI_y\left(GJ+\frac{\pi^2 EI_w}{(0.6992L)^2}\right)}$	$M_{cr0,1t}\Big/\sqrt{\left(1-\frac{EI_y}{EI_x}\right)\left(1+\frac{2EI_y}{3EI_x}\right)}$

- **Numerical solutions**

The finite element method (FEM) was used for the numerical solutions using the commercial software ANSYS APDL, since the classic LBA does not account for prebuckling deformations, it is only used for calculating M_{cr0}. To consider prebuckling deformations, an iterative process is needed that alternate between static and buckling analysis: deformations are induced by static analysis, then the beam geometry is updated, and then LBA is performed. Furthermore, GNIA was employed. The results

of these two methods were found to be identical if the iterative analysis was done correctly. That is, if the static analysis step was conducted using a nonlinear analysis. This is because the nonlinear analysis captures the true curvature of the beam by applying the load incrementally. Generally, it was found that 10 sub-steps in the static analysis result in reasonably good results.

As for the FEM models, both beam and shell element models were created, but it was found that special considerations need to be taken for how to define the supports. If the prebuckling deformations are to be accounted for, the results are dependent on whether the supports are interpreted in the global (i.e., original, undeflected) or local (i..e, deflected) coordinate system. In beam finite element, applying twisting supports about the global z axis creates a component of rotational fixity about the local weak axis of the beam (y'). At the same time, if twisting rotational fixity is applied by adding two cantilevers at the end of the beam as shown in Fig. 3, this will create a twisting rotation fixity in the local coordinate system, even after the beam deflects. Since in the analytical derivations the supports are interpreted in the local coordinate system, the latter approach is followed in the finite element models.

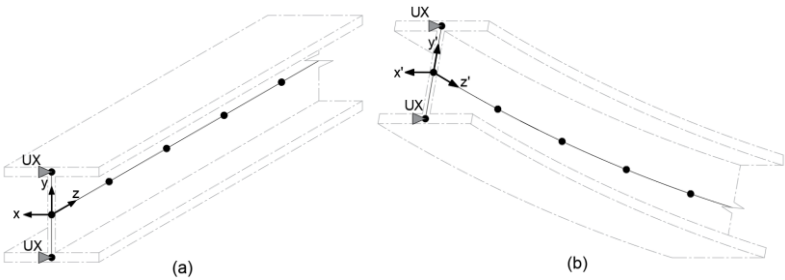

Figure 3: Support against local twisting rotation: (a) undeformed, (b) deformed.

In the shell element, global supports along the global y-axis create a problem when applying the moment as distributed pressures at the edges of the beam, since they take a component of the load as the beam deflects. To solve this problem, supports as shown in Fig. 4 are used. To reduce the localized deformations, all the nodes are restrained against twisting rotation, by introducing a master node which all the nodes at the end of the beam are rigidly linked to. These settings are for the PrPw end. To induce warping fixity, the nodes in the rigid region follow the master node in the (UX) as well, and to induce rotational fixity, the master node is restrained against (ROTY).

Figures 5-9 show the results of the various end support conditions using the different numerical and analytical methods. The figures show the increase in moment (i.e., difference between M_{cr} and M_{cro}) for the different boundary conditions. (Note, GNIA has been performed for DSI sections only. Also, FrPw-FrPw support case has not been considered in shell FEM). The results show that there is a significant difference between the DSI and RHS sections, with RHS sections generally having higher effect of prebuckling deformations (but the results are also affected by the end supports).

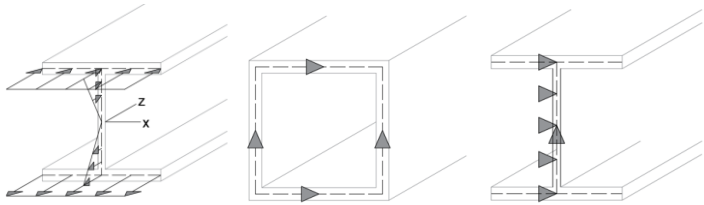

Figure 4: End supports and loading in shell FE model

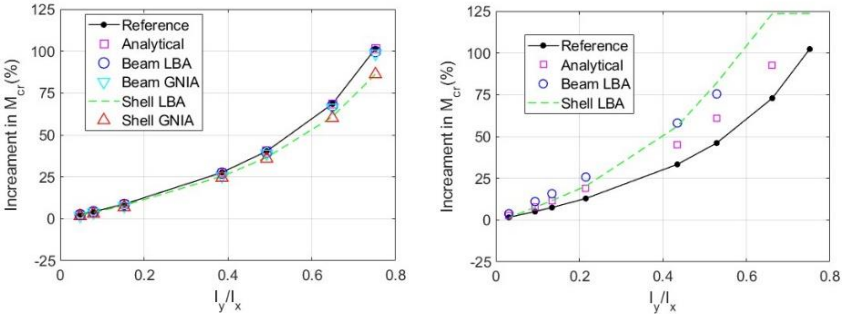

Figure 5: Critical moment increase, PrPw-PrPw, DSI (left) and RHS (right)

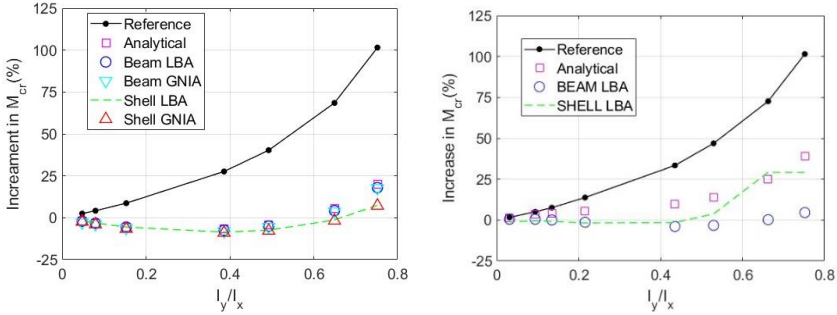

Figure 6: Critical moment increase, FrFw-FrFw, DSI (left) and RHS (right)

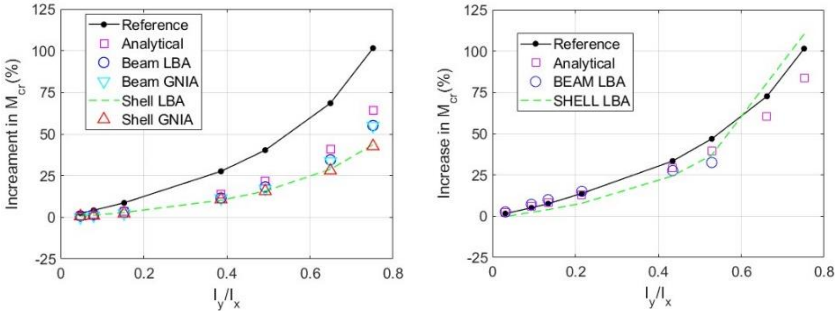

Figure 7: Critical moment increase, PrPw-FrFw, DSI (left) and RHS (right)

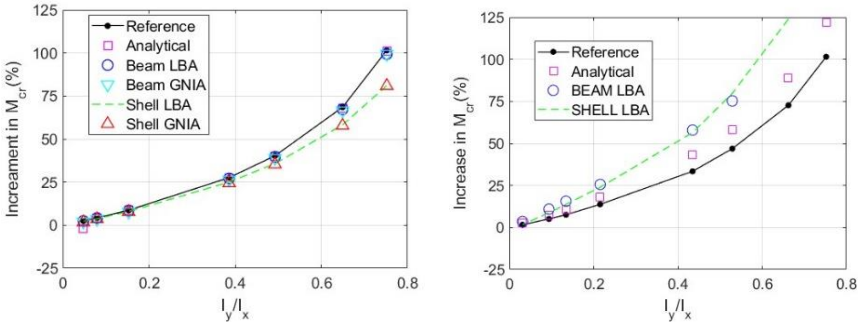

Figure 8: Critical moment increase, PrFw-PrFw, DSI (left) and RHS (right)

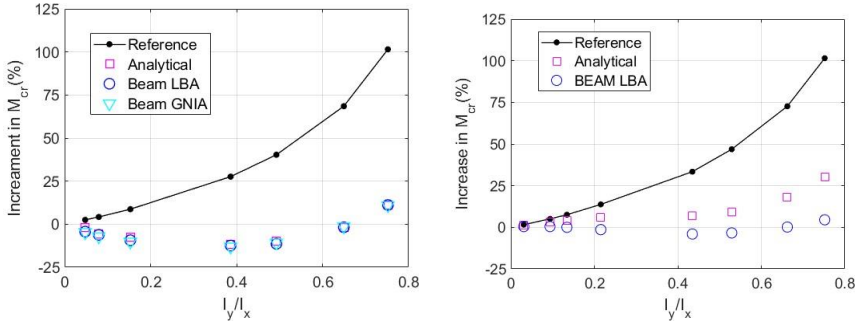

Figure 9: Critical moment increase, FrPw-FrPw, DSI (left) and RHS (right)

Regarding end supports, they have an imoprtant influence on the effect of prebuckling deformations. It is clear that rotation fixity has much higher effect than that of warping fixity. It is to highlight that in certain support conditions there is a decrease rather than an increase, i.e., the prebuckling deflection can decrease the critical moment,

unlike what is suggested in the literature. Regarding the different methods, generally good agreement between the methods is observed, but the agreement is better in the case of DSI than RHS. This is because the applied displacement approximations are less appropriate for sections with large torsional rigidity. Finally, the shell model results can be different from those from the other methods, especially for RHS sections, due to the localized deformations which are always present in shell FEM but excluded from beam models.

- **Summary**

In this chapter, closed formed solutions for the critical moment of beams considering prebuckling deformations, torsional rigidity, and various end support conditions were derived using the energy method. Furthermore, various numerical FEM studies were conducted to validate the analytical solutions. It was found that in general the results of the various methods agree, but certain considerations need to be taken if prebuckling deformations are considered. In the analytical solutions, it is sometimes important to include multiple terms in the shape functions used in the derivation to properly capture the critical moment. In the numerical studies, the boundary conditions in the FEM models (both beam and shell) need to be defined properly so that they remain in the local-axis coordinates. Regarding the effect of end supports, it was found that it significantly influences how prebuckling deformations impact the critical moment — and in some cases, this influence can even be negative.

4. The effect of intermediate supports

The next effect to be studied is the effect of intermediate lateral and torsional supports. Since the beam element was shown to effectively predict the results, it was solely used in the analysis. Moreover, as the iterative LBA method produced results identical to those obtained from GNIA, LBA was employed for critical moment calculations, while GNIA was limited to shape analysis. The analyses were also limited to DSI sections. Four types of intermediate lateral supports are introduced as: Top flange Lateral Support (TLS), Centroid Lateral Support (CLS), Bottom flange Lateral Support (BLS), and All section Lateral Support (ALS), the latest introducing support against the twisting rotation. Similar cross sections and material as in the previous Chapter were used, with beam lengths ranging from 2.5-50 meters to study the length effect. The intermediate supports were applied to the beam elements using vertical cantilevers with length equal to half the beam depth, as shown in Fig. 10.

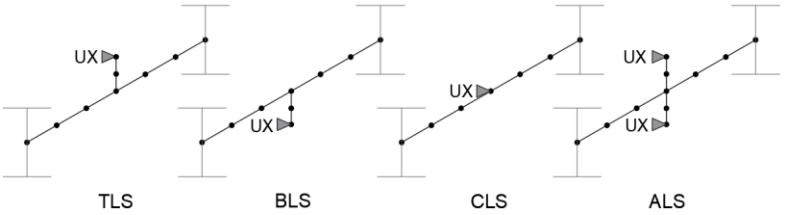

Figure 10: Intermediate lateral support types applied on the beam element.

- **Effect of intermediate support types**

Figure 11 shows the effect prebuckling deformations on beams with the different types of intermediate lateral supports. The ALS curve follows the reference curve (with no intermediate supports). Other types of intermediate supports follow the reference curve for deeper beams, but have a sudden change in the curve at a certain I_y/I_x value (depends on the type of intermediate support), with TLS having the highest value, then CLS, and finally BLS. The effect can even be negative in some cases.

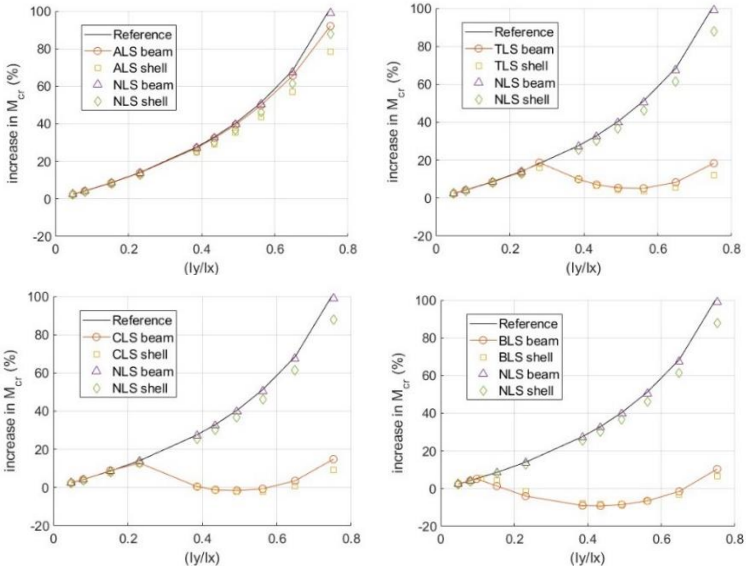

Figure 11: Effect of intermediate lateral supports.

- **Beams with intermediate lateral supports and various lengths**

Figures 12 and 13 show the results for beams with various lengths. The length has a significant effect on how the critical moment is changed by the prebuckling deformations, as it both changes the I_y/I_x value of which the curves switch into a different behavior, as well as changes the values within the curves. TLS shows a decrease in I_y/I_x threshold for reference behavior with longer beams, while CLS shows an increase, and BLS has a more irregular behavior. It is to note that significant decreases in critical moment can be experienced in certain cases.

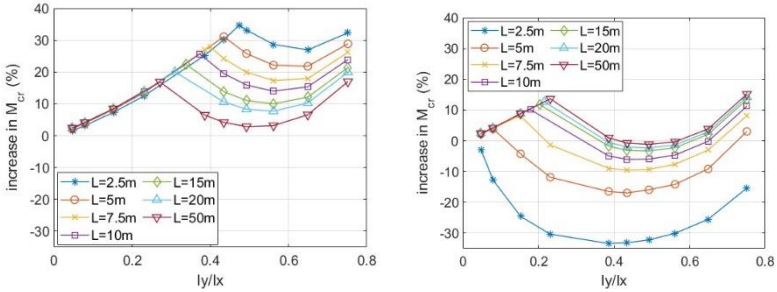

Figure 12: Effect of beam length on the moment increase: TLS (left) and CLS (right).

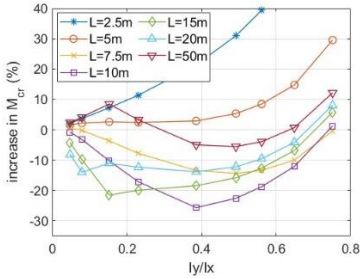

Figure 13: Effect of beam length on the moment increase: BLS.

- **The combined effects of intermediate supports and end supports**

Previously, the effect of end supports was studied, and then the effect of intermediate supports. This section combines these two effects with each other. Figures 14 and 15 show the increase in critical moment for the different end and intermediate support cases. In general, the results show the same trends of the effect of end supports as those obtained for beams without intermediate lateral support. Furthermore, the

results also show the same trends for the effect of intermediate support. The combined effect of intermediate and end supports can cause a decrease in critical moment of up to 35% for the investigated case (and can be even higher for shorter beams).

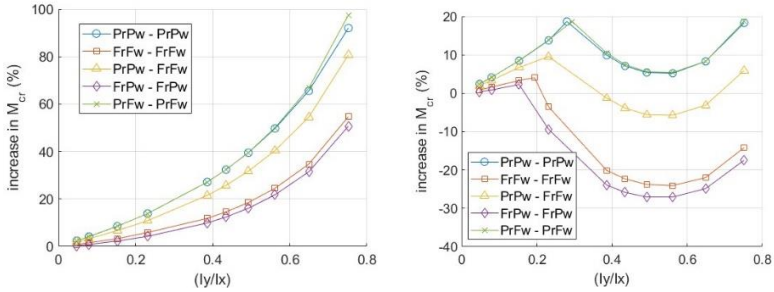

Figure 14: The effect of end supports: ALS (left) and TLS (right).

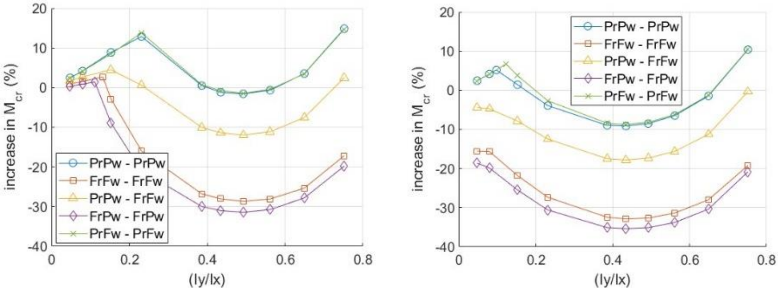

Figure 15: The effect of end supports: CLS (left) and BLS (right).

- **Analytical studies**

It was repeatedly seen in previous sections that when introducing intermediate supports, the moment increase curves usually have two parts. This phenomenon can be explained by the buckling shapes (the shape can vary depending on the case). An analytical study is presented to understand this. Similar to the previous chapter, the energy method is employed, but the derivations are limited to the PrPw-PrPw end conditions to reduce complexity. Five candidates for the displacement functions are defined, and referred to from (a) to (e).

It is to observe that Shape (a) is point-symmetric, with two longitudinal half-waves in both u and φ, while the others are symmetric with one or three half-waves. In (a) and (b), u and φ are zero at mid-span; in (c), (d), and (e), u is zero at some cross-

section, but φ is non-zero at mid-span. Depending on lateral support positions, some shapes are kinematically possible, others not. This also needs to be taken into consideration when selecting the proper shape function. The analytical prediction for the lowest critical moment is the minimum among those that belong to the kinematically admissible shapes. During the derivations, similar assumptions for open sections as was introduced in Chapter 2 are used. Following the shape functions presented, five critical moment formulae are given (but are not shown here).

Table 2 shows numerical results using both analytical and numerical solutions for two lengths (5 and 30m) and for various beam depths. The analytical results agree well with the beam model results. Regarding the shapes in the case of ALS, shape (a) leads to the lowest critical moment values. Moreover, in many cases the buckled shapes without and with prebuckling deflection are different, i.e., there is mode switch. The results show that sometimes the classic LTB shape is point-symmetric, which switches to a symmetric one, see e.g., the CLS type; however, in other cases the classic LTB shape is symmetric, but can be switched to point-symmetric, see e.g., BLS type. Since the nature of the buckled shapes, and especially the mode switch seems to have crucial role in the value of moment increase, a shape analysis study is conducted.

Table 2: Analytical results

L	mm	5000	5000	5000	5000	30000	30000	30000	30000
h	mm	500	300	200	150	500	300	200	150
I_y/I_x		0.05	0.15	0.39	0.75	0.05	0.15	0.39	0.75
$M_{cr0}^{(a)}$	kNm	2340	1554	1213	1071	175	161	155	152
$M_{cr0}^{(b)}$	kNm	4573	2870	2092	1749	265	236	224	218
$M_{cr0}^{(c)}$	kNm	90510	54440	36515	27626	2712	1785	1354	1153
$M_{cr0}^{(d)}$	kNm	6562	5101	4526	4296	757	715	694	683
$M_{cr0}^{(e)}$	kNm	750	642	670	749	218	290	358	407
$M_{cr}^{(a)}$	kNm	2398	1688	1548	2159	179	175	197	305
$M_{cr}^{(b)}$	kNm	4616	2976	2390	2896	267	244	255	361
$M_{cr}^{(c)}$	kNm	19165	4678	1798	1400	695	277	173	181
$M_{cr}^{(d)}$	kNm	3045	1515	1017	1099	351	212	156	175
$M_{cr}^{(e)}$	kNm	763	659	687	967	184	165	142	169

M_{cr0}^{ALS}	kNm	2340 a	1554 a	1213 a	1071 a	175 a	161 a	155 a	152 a
M_{cr}^{ALS}	kNm	2398 a	1688 a	1548 a	2159 a	179 a	175 a	197 a	305 a
increase	%	2.48	8.65	27.61	101.5	2.48	8.65	27.61	101.5
inr, FEM	%	2.21	8.23	26.69	95.67	2.43	8.51	27.14	92.06
M_{cr0}^{TLS}	kNm	2340 a	1554 a	1213 a	1071 a	175 a	161 a	155 a	152 a
M_{cr}^{TLS}	kNm	2398 a	1688 a	1548 a	1400 c	179 a	175 a	173 c	181 c
increase	%	2.48	8.65	27.61	30.72	2.48	8.65	11.75	19.60
inr, FEM	%	2.21	8.23	26.62	28.78	2.44	8.48	9.93	18.36
M_{cr0}^{CLS}	kNm	2340 a	1554 a	1213 a	1071 a	175 a	161 a	155 a	152 a
$M_{cr}^{CLS}0$	kNm	2398 a	1515 d	1017 d	1099 d	179 a	175 a	156 d	175 d
increase	%	2.48	-2.51	-16.18	2.62	2.48	8.65	0.95	15.35
inr, FEM	%	2.21	-4.25	-16.48	2.14	2.46	8.87	0.52	14.87
M_{cr0}^{BLS}	kNm	750 e	642 e	670 e	749 e	175 a	161 a	155 a	152 a
M_{cr}^{BLS}	kNm	763 e	659 e	687 e	967 e	179 a	165 e	142 e	169 e
increase	%	1.69	2.63	2.53	29.14	2.48	2.76	-8.23	11.66
inr, FEM	%	1.6	2.63	2.91	29.55	2.44	1.42	-8.96	10.39

- **Shape analysis**

To better understand the mode switch, the results are first analyzed in detail, focusing on when the mode switch occurs and how the buckled shapes differ depending on whether the switch happens or not. The results are visualized in Fig. 16, where the letter P indicates a point symmetric, and S indicates a symmetric shape. Each case gets two letters, the one on the left is when no prebuckling deformations are considered, and the one on the right is with prebuckling deformations. For an example, PS refers to the case when the shape is point symmetric without prebuckling deformations, and symmetric when prebuckling deformations are introduced, meaning that during the loading, the beam starts with a point symmetric shape, then shifts to a symmetric one.

Several observations can be made. In the cases of TLS and CLS, the left parts of the curves belong to PP, while the right (quasi-parabolic) parts of the curves belong to PS. The I_y/I_x threshold where the two lines join, i.e., where the behavior changes from PP to PS, is dependent on the length, and the trends are similar to what was observed in the length study.

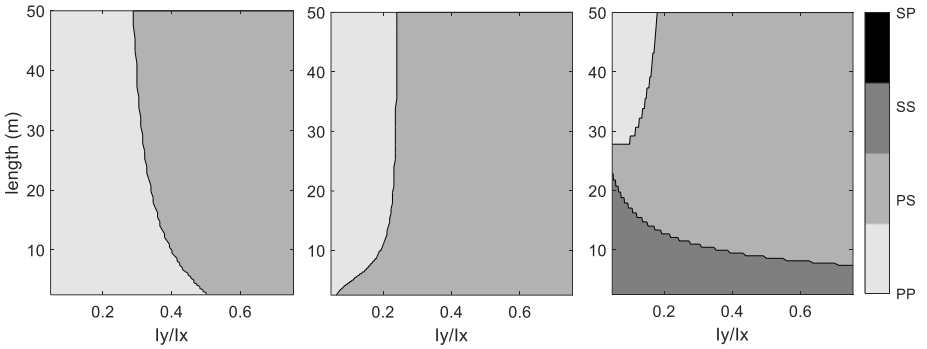

Figure 16: Overview of buckling shapes (left: TLS, middle: CLS, and right: BLS).

The most complex case however is BLS (which was also the experience earlier). If the beam is long and the I_y/I_x is large, then the behavior is PS. When the beam is extremely long and I_y/I_x is small, the behavior is PP. For shorter beams, the behavior is SS, which means the buckling mode is symmetric either the prebuckling deflection is considered or not for low I_y/I_x ratios. These different cases can be shown in detail using the GNIA method, where an initial imperfect shape is defined based on the buckling analysis (using the first mode), and then the shapes are captured for various sub steps during the nonlinear analysis, as shown in Figs. 17-18. One interesting case was found in the CLS support, where two mode switches happen, starting from point symmetric, to symmetric, and then to point symmetric again, giving the PSP case.

- **Summary**

The effect of intermeidate lateral supports was investigated in this chapter. It was found that the intermediate lateral supports have a signifnat influence on the prebuckling deformation effect, since they affect the buckled shape of the beam. The buckled shape can be either symmetric or point-symmetric, and can be different for the same beam depending on whether or not the prebuckling deformations are consiered, suggesting a mode switch during the loading. The effect of prebuckling deformations has a wide range as result, ranging between an increase of up to more than 80%, to a decrease of up to 40% depending on: (i) type of intermediate support, (ii) the length of the beam, (iii) the depth of the beam, or (iv) the end supports.

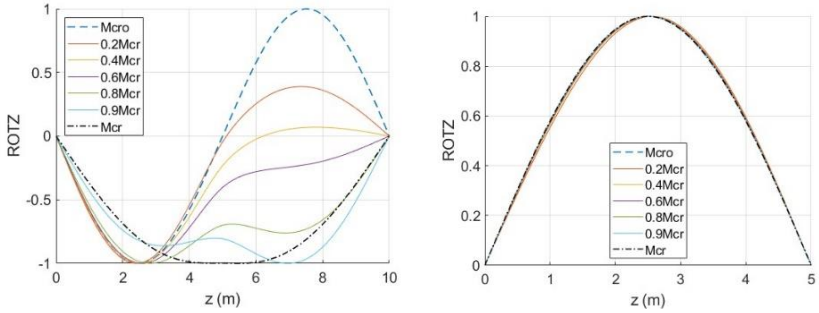

Figure 17: Shape analysis cases: PS (left), SS (right)

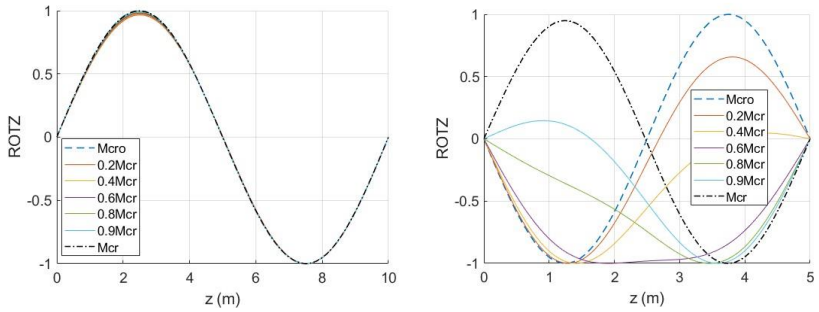

Figure 18: Shape analysis cases: PP (left), PSP (right)

5: Thesis Statements

- **Thesis 1**

I have conducted an analytical study on the lateral torsional buckling of beams considering the prebuckling effect. I have summarized most of the available analytical formulae in the literature, highlighting the variations between them (even for the seemingly same case), showing that the solution is far from unambiguous. I rederived the different formulae, identifying the important factors in the analytical derivations which influence the critical moment formula. By doing so, I explained the differences between the formulae found in the literature. Furthermore, by doing the analytical study, I showed that several further variants can be derived (but not all of them are accurate). I defined the requirements for the approximations and when it is appropriate to do them. I have distinguished between cross sections with high and low torsional rigidities in the

analytical derivations. By doing so, I have shown that the torsional rigidity of the section has an important, but unexplored effect, that is why open and closed section beams are differently affected by the prebuckling effect [AGA1, AGA4].

- **Thesis 2**

I have conducted a numerical study for the validation of the analytical solutions. For that purpose, I developed beam and shell finite element models, which are suitable for considering the prebuckling deformations. I pointed out some important modelling aspects that have (or might have) significant influence on the results when LTB with prebuckling effect is studied. I have shown that classical models used for LBA might not be suitable for an FEM analysis that consider prebuckling deformations, and special considerations must be made in order for the results to be comparable with the analytical solutions (namely: loading application, supports in beam and shell FEM models, and nonlinear static analysis in iterative LBA) [AGA2].

I have used two types of analysis for the numerical solutions. First, I proposed an iterative LBA methods that alternate between static analysis for inducing prebuckling deformations, and linear buckling analysis that obtain a critical moment value. I have shown that convergence occurs, leading to critical moment value that's close to the analytical solutions. I have shown that using a linear analysis in the static analysis step produces error, and non-linear analysis lead to better results. Then, I have conducted GNIA with very small imperfections, leading to critical moment values that are very close to the results from iterative LBA method, validating the use of such an algorithm. I have compared the shell and beam FEM methods, highlighting that the effect of non-beam-like deformations is significantly magnified when prebuckling deformations are considered [AGA2, AGA4].

- **Thesis 3**

I have considered other boundary conditions than the simple forked support case which was mostly discussed in the literature. I have derived closed formed analytical solutions for various boundary conditions, and I have created numerical models for these different boundary conditions cases. I have conducted a parametric study using the proposed analytical and numerical solutions. I compared the results from these methods accounting for the combined effects of (i) prebuckling deformations, (ii) boundary conditions, and (iii) torsional rigidity [AGA2, AGA5, AGA6].

Using the results, I have shown that the different methods used agree to an acceptable degree, validating the derived analytical solutions for most cases, with some inaccuracies, especially when rotational fixities are introduced. I have shown that the source of these inaccuracies is the approximative nature of the shape functions used. I have derived enhanced solutions based on more accurate shape functions, giving more accurate results. I have shown that the end supports have a significant effect on how the prebucking deformations influence the solution, highlighting that proposed formulae in the literature are only valid for the simple forked support case.

I have shown that unlike what is suggested by literature, the effect of prebuckling deformations is not always positive, and can be negative in certain support cases. I have shown that the length of the beam influences the solution in some boundary condition cases, which is present in the FEM solution, but can only be captured in the analytical solution if the enhanced shapes are used. I have shown that longer beams require more terms in the shape functions to produce accurate results. I have shown that the effect of non-beam-like deformations in the shell element solution is further heightened when fixity is introduced to the twisting rotation at the end of the beam [AGA2, AGA6].

- **Thesis 4**

I have considered the intermediate lateral and torsional supports, I have derived analytical closed formed solutions for the critical moment of beams considering prebuckling deformations for four cases: (i) lateral support at the top flange (ii) lateral support at the bottom flange (iii) lateral support at the centroid, and (iv) lateral support with twisting rotation fixity. I have created numerical models for these cases and conducted a parametric study using the various methods [AGA3, AGA7].

Using the results, I have shown that the location of the intermediate support has a drastic effect on how the prebuckling deformations affect the solution. The differences can vary between a significant increase in the critical moment to a significant decrease (compared to the case when prebuckling deformations are not considered) depending on which kind of intermediate support is used. I have shown that the reason for these discrepancies is in the buckling shape, which vary depending on the type of intermediate support. I have shown using both the LBA and the analytical solutions that the buckling shape can differ depending on whether or not the prebuckling deformations are considered, suggesting the presence of a ‘mode switch’ as the load increases.

I have further investigated the mode switch behavior using the GNIA method, plotting and observing the transitioning from one mode to another during the non-linear analysis, and confirming the mode-switch phenomena. I have investigated the effect of the initial shape and initial imperfection value on the mode-switch, showing that if the initial imperfection value is small, the beam will always switch to the same shape regardless of the initial shape, but larger initial imperfection values affect the final shape as well as the critical moment value. Finally, I have studied the practical effectiveness of the use of intermediate lateral supports, highlighting the variations between little to know advantage, to high advantage, depending on the type of the intermediate support, the cross section, and length of the beam [AGA3, AGA7].

5. Publications

Journal Papers

[AGA1] Abureden. G.A., Adany, S. (2025). The Effect of Torsional Rigidity and Approximations in Analytical Solutions for the Critical Moment of Beams Considering Prebuckling Deflections. *Periodica Polytechnica Civil Engineering*.

[AGA2] Abureden. G.A., Adany, S. (2025). Influence of prebuckling deflections on the elastic lateral-torsional buckling of thin-walled beams with various end supports: analytical and numerical investigations in the case of doubly-symmetric cross-sections. Thin-Walled Structures, 113025

[AGA3] Abureden. G.A., Adany, S. (2025). Elastic lateral-torsional buckling of single-span doubly symmetric I-section beams with intermediate discrete lateral support considering prebuckling deflections. Thin-Walled Structures, 113179.

Conference Papers

[AGA4] Abureden. G.A., Adany S. (2023). The effect of prebuckling deflections on the lateral-torsional buckling of beams: numerical studies. *ce/papers*, *6*(3-4), 1686-1690..

[AGA5] Abureden. G.A., Adany S. (2023). On the effect of prebuckling deflections on the lateral-torsional buckling of beams. Proceedings of the Ninth International Conference on Thin-Walled Structures (ICTWS2023), Nov 29 – Dec 1, 2023, Sydney, Australia.

[AGA6] Abureden. G.A., Adany S. (2024). Critical moment of doubly-symmetric beams with prebuckling deflection: The effect of end supports. In Proceedings of the Annual Stability Conference, Structural Stability Research Council. San Antonio, Texas.

[AGA7] Abureden. G.A., Adany S. (2024). Critical moment of doubly-symmetric beams with prebuckling deflection: The effect of intermediate supports. In Proceedings of the Annual Stability Conference, Structural Stability Research Council. Louisville, Kentucky.

6. References

[1] Clark J.W., Knoll A.H. (1958) „Effect of deflection on lateral buckling strength", J. Eng. Mech. Div. ASCE, 84(2), pp. 1596-1–1596-18.

[2] Vacharajittiphan, P., Woolcock, S.T., Trahair, N.S. (1974) „Effect of in-plane deformation on lateral buckling", Journal of Structural Mechanics, 3(1), pp. 29-60.

[3] Pi Y.L., Trahair N.S. (1992) „Prebuckling Deflections and Lateral Buckling. I: Theory", J. Struct. Eng. Vol. 118. pp. 2949-2966.

[4] Trahair N.S. (1993) „Flexural-Torsional Buckling of Structures", Chapman and Hall, London, 1993.

[5] Torkamani M.A.M (1998) „Transaformation matrices for finite and small rotations", Journal of Engineering Mechanics, 124(3), pp. 359-362.

[6] Mohri, F., Potier-Ferry, M. (2006) „Effects of load height application and pre-buckling deflections on lateral buckling of thin-walled beams", Steel and Composite Structures, Vol 6, No 5, pp. 1-15.

[7] Torkamani M.A.M., Roberts E.R. (2009) „Energy equations for elastic flexural–torsional buckling analysis of plane structures", Thin-Walled Structures, Vol 47, pp. 463-473.

[8] Attard, M.M., Kim, M-Y. (2010) „Lateral buckling of beams with shear deformations – A hyperelastic formulation", Int Journal of Solids and Structures, Vol 47, pp. 2825-2840.

[9] Erkmen, R.E., Attard, M.M. (2011) „Lateral–torsional buckling analysis of thin-walled beams including shear and pre-buckling deformation effects", Int Journal of Mechanical Sciences, Vol 53, pp. 918-925.

[10] Mohri, F., Damil, M., Potier-Ferry, M. (2012) „Pre-buckling deflection effects on stability of thin-walled beams with open sections", Steel and Composite Structures, Vol 13, No 1, pp. 71-89.

[11] Pezeshky, P., Mohareb, M., (2018) „Distortional lateral torsional buckling of beam-columns including pre-buckling deformation effects", Computers and Structures, Vol 209, pp. 93–116.

[12] Su Y., Zhao H., Liu S., Li R., Wang Y., Wang Y., Bian J., Huang Y. (2019) „Buckling of beams with finite prebuckling deformation", International Journal of Solids and Structures, Vol 165, pp. 148-159.

[13] Zhang, F., & Kim, M. Y. (2025). A simple but accurate FEM for lateral-torsional buckling loads of mono-symmetric thin-walled beams considering pre-buckling effects. Thin-Walled Structures, 206, 112676.